Multinucleon transfer reactions in the $^{40}Ca+^{124}Sn$ system studied via γ-particle coincidences

L. Corradi, G. de Angelis, A. Gadea, G. Maron, D. R. Napoli, and A. M. Stefanini
Istituto Nazionale di Fisica Nucleare, Laboratori Nazionali di Legnaro, Via Romea 4, I-35020 Legnaro, Padova, Italy

S. Beghini, D. Bazzacco, G. Montagnoli, P. Pavan, F. Scarlassara, and C. A. Ur
Dipartimento di Fisica, Universitá di Padova, and Istituto Nazionale di Fisica Nucleare, Sezione di Padova, Via Marzolo 8, I-35131 Padova, Italy

J. H. He
Shanghai Institute of Nuclear Research, Shanghai 201800, China

C. Fahlander
Physics Department, Lund University, S-22100 Lund, Sweden

G. Pollarolo and F. Cerutti
Dipartimento di Fisica Teorica, Universitá di Torino, and Istituto Nazionale di Fisica Nucleare, Sezione di Torino, Via Pietro Giuria 1, I-10125 Torino, Italy

(Received 17 September 1999; published 19 January 2000)

Multinucleon transfer reactions have been investigated in the system $^{40}Ca+^{124}Sn$ at $E_{LAB}=170$ MeV. The setup was the GASP multidetector array and two bidimensional position sensitive parallel plate detectors, from which γ-particle and γ-γ-particle coincidences were taken for a large variety of transfer channels. Differential and total cross sections to the lowest excited levels of the heavy and light nuclei produced in the transfer process have been measured down to the $-4p$ channel. A comparison with a first-order complex WKB Born approximation for the $+1n$ and $-1p$ transfer channels has been done, showing an overall good agreement with the data.

PACS number(s): 25.70.Hi, 24.10.−i, 21.10.−k

I. INTRODUCTION

Precision measurements of heavy-ion transfer reactions to the excited levels of the final products provide invaluable information for both nuclear structure and reaction dynamical studies. From the spectroscopic point of view, such reactions are particularly useful in that they allow one to populate regions of isospin, spin, and excitation energy not accessible by other means [1,2]. From the point of view of the reaction mechanisms, especially at energies close to the Coulomb barrier, transfer reactions are important to investigate which degrees of freedom are relevant in the grazing regime, i.e., single nucleon, pair or more complicated transfer modes [3–12]. The relation of these channels to other competing mechanisms, like sub-barrier fusion, is one of the most interesting and still not well understood problems in low-energy nuclear physics. It is in fact well known [13,14] that transfer channels may represent an important doorway state for the enhancement of sub-barrier fusion cross sections. To have a quantitative explanation of those effects one needs the form factors for the relevant channels and these can only be determined from the measurement of the cross sections to individual final states of the reaction products.

For resolving the γ-ray transitions between individual levels of the produced nuclei it is necessary to use Ge detectors. Experiments in this field received a significant boost after the large γ-detector arrays became available [15,16]. Efficient population of neutron-rich nuclei has been demonstrated for instance in the determination of the level scheme of ^{68}Ni [17] and in Ref. [18]. The impact parameter dependence of the transfer strength can be studied using suitable particle detectors to tag the γ radiation and to perform the Doppler correction. Parallel-plate detectors (PPAC) have been used in several works to study high spin states populated in heavy-ion transfer reactions [19,20], transfer probabilities at large radial separation [21,22] and particle correlation in nuclear media [23–27].

In most of the experiments done so far with γ detectors triggered by particle detectors, single γ-particle coincidences have been taken, and studies have been restricted to one- and two-nucleon transfer reactions. In the present work we used the GASP γ-ray detector array [15] and two PPAC [28] to study multinucleon transfer in the reaction $^{40}Ca+^{124}Sn$ at $E_{LAB}=170$ MeV. This system was recently investigated to extract the inclusive transfer cross sections [10] and the sub-barrier fusion cross sections [29]. In Ref. [10], by using a time-of-flight magnetic spectrometer, reaction channels have been identified up to the pickup of six neutrons and the stripping of six protons and the *Q*-value integrated cross sections for the final transfer products have been measured.

The aim of the present measurements was to extract the differential and total cross sections for the lowest excited levels of the transfer products. The comparison with theoretical calculations, at least for the simple one-particle transfer processes, allows the extraction of the single-particle form factors that constitute the fundamental ingredient for more elaborate coupled-channels calculations [6,7].

The paper is organized as follows: in Sec. II we present

the setup, in Sec. III we present the experimental results, in Sec. IV we compare the experimental and theoretical differential and total cross sections for the one-particle transfer channels. Conclusions will be given in Sec. V.

II. THE SETUP

The experiment has been performed at the XTU Tandem accelerator of the Laboratori Nazionali di Legnaro. A ^{40}Ca beam has been extracted as a CaH_3^- molecule from an ion sputter source and delivered at 170 MeV, with an intensity of 1–2 *p*nA, onto a ^{124}Sn target with a thickness of 180 μg/cm^2 and an isotopic enrichment of 99.8%. The target was placed at 45° with respect to the beam direction and in the center of a 1 mm thick aluminum spherical chamber installed inside the GASP array. Two rectangular parallel-plate detectors of the multiwire-type (MWPPAC's) (see Ref. [28] for details), with an active area of 10×8 cm^2 each, have been placed inside the chamber symmetrically around the target (with the anode planes parallel to the beam direction) at a distance of $\simeq 7$ cm. The MWPPAC's, which were operated independently, have been used to get the angular distributions of the transfer products and to allow Doppler correction of the γ radiation.

With the present geometry the total solid angle was $\simeq 3$ sr. The in-plane ($\theta_{\rm LAB}$) and out-of-plane ($\phi_{\rm LAB}$) angular ranges were $56° \leqslant \theta_{\rm LAB} \leqslant 120°$ and $-40° \leqslant \phi_{\rm LAB} \leqslant +40°$. The transfer products are peaked at the grazing angle $\theta_{\rm LAB} \simeq 75°$ with an angular distribution width $\simeq 25°$, and it was possible to integrate $\simeq 36\%$ of the total transfer flux. To allow only the light ejectiles to reach the detectors, a thin ($\simeq 300$ μg/cm^2) Ni foil was placed in front of the MWPPAC covering the angular range $56° \leqslant \theta_{\rm LAB} \leqslant 90°$. This was done to prevent a too high count rate due to the elastically scattered heavy recoils at $\theta_{\rm LAB}$ smaller than 90°, and to help stopping bursts of δ electrons from the target. The fact that only the light ejectiles triggered the detectors helped to cleanup the γ spectra obtained after Doppler correction. The intrinsic efficiency of the MWPPAC was 100% for the detected ions over the whole surface, and has been tested with calibration runs before and after the experiment.

The GASP array was used in its full configuration, i.e., with 40 Ge detectors placed at $\simeq 27$ cm from the target, and with the BGO inner ball which provides the fold (which is related to the multiplicity through the detector response function) and the sum energy of the γ cascade. The photopeak efficiency of the Ge array was $\simeq 5\%$ for the γ transitions with energies of $\simeq 650$ keV, while the efficiency of the BGO ball was $\simeq 80\%$. The counting rate in the Ge detectors was $\simeq 1$ kHz. For the acquisition we required a coincidence between an event in a MWPPAC and at least one γ ray in the Ge or BGO detectors. Besides the X and Y positions of the MWPPAC, the energy of each Ge, the fold and the sum energy of the inner ball, also the time-of-flight between MWPPAC-Ge, MWPPAC-BGO, and Ge-BGO were accumulated and stored on tape.

III. EXPERIMENTAL RESULTS

Transfer products have been identified through their characteristic γ transitions, almost all of which were known from literature [30]. Knowing in each event the θ and ϕ angles in the MWPPAC and the angular position of the Ge detector, Doppler correction can be applied to the detected γ rays. Since the coincident γ radiation could come from the light or from the heavy partner, the Doppler correction for each Ge detector has been done twice (once for the light and once for the heavy partner). The events corresponding to the wrong Doppler correction create broad peaks in the γ spectra, which, being distributed over several channels (see, e.g., Fig. 3 below), do not reduce significantly our sensitivity. The routine for the Doppler correction takes into account the first-order Doppler effect and does not correct for the *Q* value of the reaction. These simplifications are suitable for the heavy partner, since its average v/c is as low as $\simeq 0.03$, hence the energy resolution of the final spectra ($\simeq 3.5$ keV at $E_\gamma \simeq 600$ keV) is good enough. For the light partner the average v/c is $\simeq 0.07$ and the width of the γ lines is larger, but still good enough for our purposes.

The γ transitions of the transfer products have different multipolarities and, in general, angular correlation effects should be considered. However, since the sum of all the spectra in the 40 Ge detectors has been taken for extracting the total yields, angular correlation effects are washed out due to the spherically symmetric geometry of the Ge array. To obtain the final Ge spectra gates have been set on the time distributions of the Ge-MWPPAC and BGO-MWPPAC events, in order to minimize the background and spurious events.

For each of the two reaction partners, two kinds of Ge spectra have been produced: the single γ spectra (GS), i.e., those simply in coincidence with an event in the MWPPAC, and the projected γ spectra (GP) coming from the projection of the γ-γ matrix, i.e., requiring a coincidence between at least two γ rays. To get the absolute intensities of the observed channels, the peaks in the GS spectra have been integrated. The GP spectra have been used to better separate

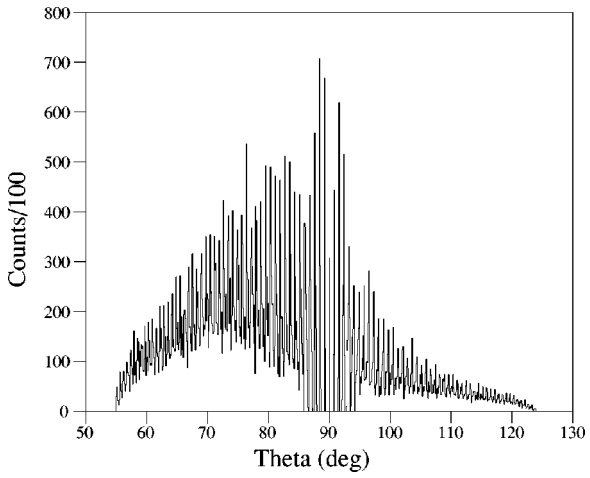

FIG. 1. $\theta_{\rm LAB}$-event distribution in the MWPPAC in coincidence with a γ transition.

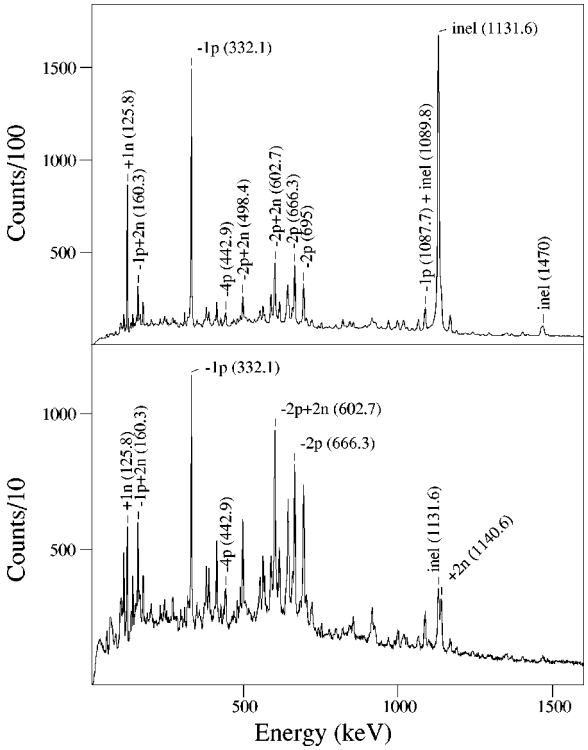

FIG. 2. Total Ge singles (top) and total projected γ-γ matrix (bottom) after Doppler correction for the heavy partner.

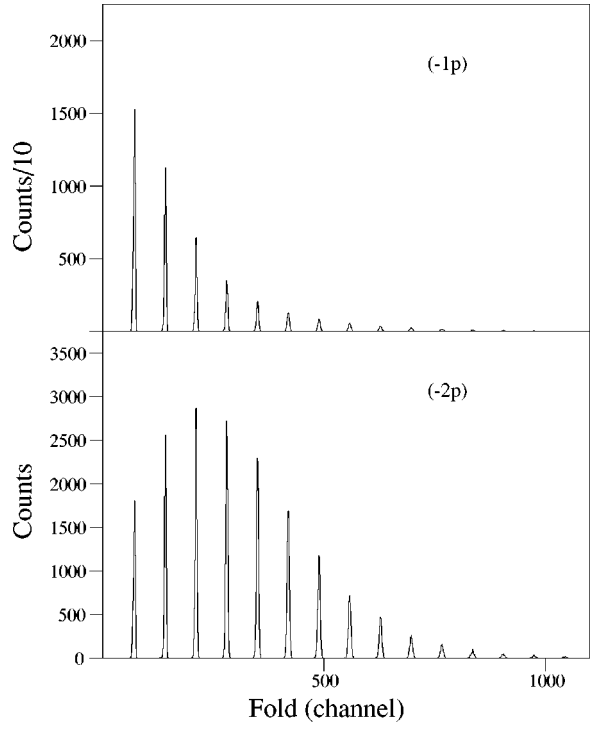

FIG. 4. Fold event distribution for the $-1p$ and $-2p$ channels after gating on the corresponding lowest transitions. Fold is related to multiplicity M_γ by the detector response function [15].

overlapping peaks and to check the correct assignment of the γ cascade to a specific nucleus.

A typical MWPPAC θ_{LAB} spectrum taken in coincidence with γ events is shown in Fig. 1. The distribution peaks at $\theta_{\mathrm{LAB}} \simeq 75°$, which is the grazing angle for the present reaction. In Fig. 2 we show the GS (top) and GP (bottom) spectra for the heavy partner, and in Fig. 3 the GS spectra for the light partner. These spectra have been produced by integrating all the events in the MWPPAC. One immediately observes the prominent peaks of the channels $+1n$, $+2n$, $-1p$, $-2p$, $-2p+2n$, with the presence of many other γ lines corresponding to the population of different excited levels. The effect of the wrong Doppler correction is clearly seen in Fig. 3 by the appearance of broad peaks. We notice the peak of the 3^--0^+ ($E_\gamma = 3740$ keV) inelastic excitation in ^{40}Ca and the prominent peak of the 2^+-0^+ ($E_\gamma = 1131.6$ keV) inelastic excitation in ^{124}Sn. This last transition is strongly suppressed in the GP spectrum (Fig. 2 bottom), thus allowing us to appreciate the presence of the lowest 2^+-0^+ transition of the $+2n$ channel.

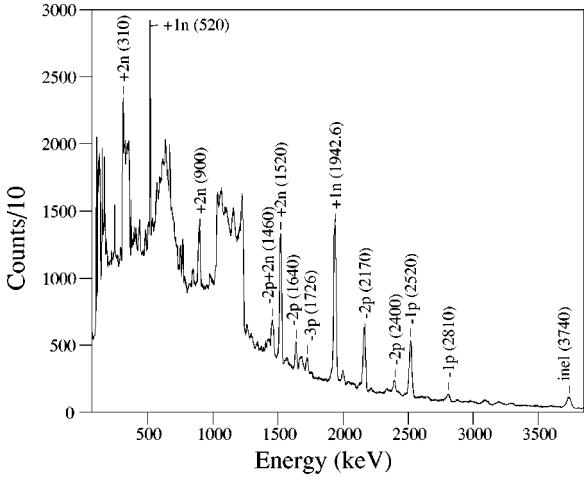

FIG. 3. Total Ge singles after Doppler correction for the light partner. Notice the presence of broad peaks corresponding to the wrongly Doppler corrected γ lines of the heavy partner.

The GP spectrum has been produced by requiring a coincidence between at least two γ rays. Therefore, the intensities of the various peaks (I_c), relative to the GS ones (I_s), depend on the Ge efficiency and on the multiplicity (M_γ) for each specific channel. In its simplest form, for a given γ transition, I_c and I_s are related by

$$I_c \simeq I_s M_\gamma \epsilon, \tag{1}$$

where ϵ is the efficiency of the γ array averaged over all transitions connected to the one of interest. Our data show that the I_c/I_s ratios get higher when considering channels involving more and more nucleons, in qualitative agreement with the increase of M_γ extracted from the BGO ball and with the increase of the average excitation energy observed in the previous experiment [10]. As an example, we show in Fig. 4 the event fold distribution for the two channels $-1p$ and $-2p$.

In Fig. 5 we show the coincidence γ-ray spectra obtained by gating on the lowest transitions of some representative transfer channels. One can appreciate the quality of the data, i.e., the possibility to detect even very weak channels, with a

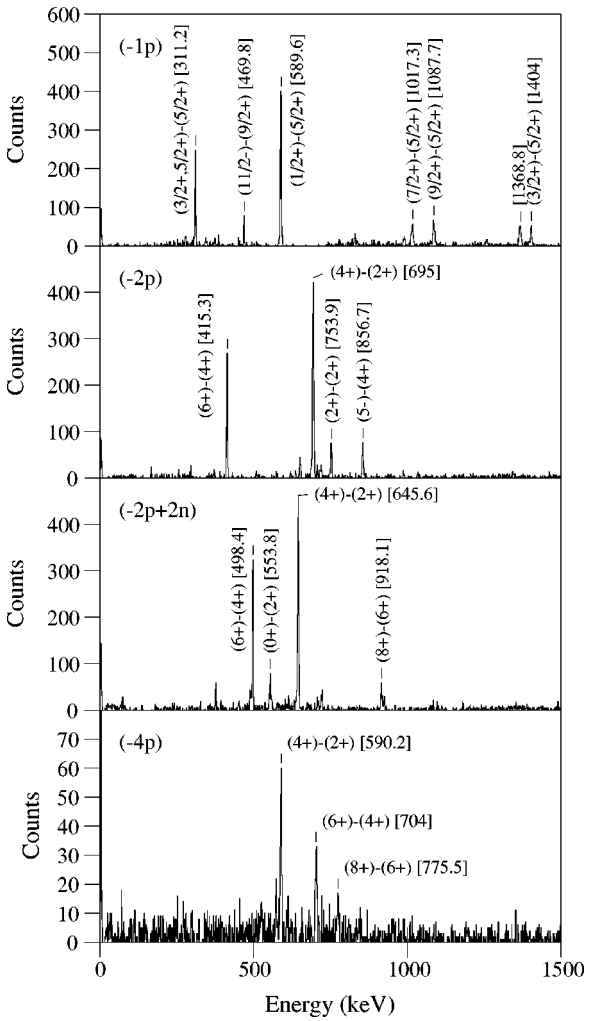

FIG. 5. Background subtracted projection of the γ-γ matrix for the heavy partner after gating on the lowest transition of the indicated transfer channels.

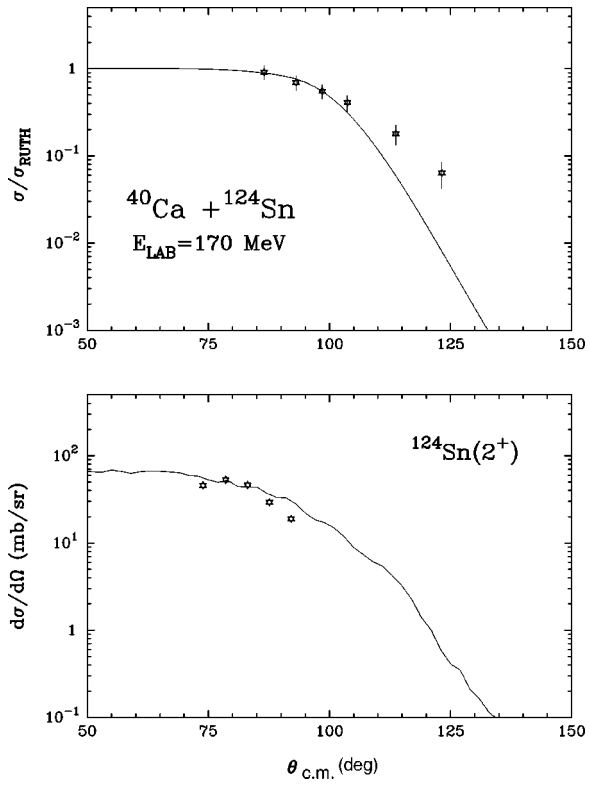

FIG. 6. Angular distribution of the elastic + inelastic channel (top) in comparison with the theoretical pure elastic angular distribution obtained with the optical potential parameters quoted in the text (the data are from Ref. [10]). At the bottom we show the angular distribution for the 2^+ inelastic excitation in ^{124}Sn in comparison with a DWBA calculation (see text).

very small background. In particular one notices the lowest γ cascade of ^{128}Xe ($-4p$ channel) up to the 8^+-6^+ transition.

In Table I we list the cross sections for all the transfer channels for which statistics allowed reliable integration of the peaks either of the lowest transition to the ground state or of the strongest one present in the GS spectra. The numbers have been corrected for the efficiencies of the Ge detectors after a calibration run with ^{152}Eu and ^{56}Co sources. To get the absolute value of the cross sections, we have chosen to normalize the intensity of the lowest 2^+-0^+ transition of ^{124}Sn to a DWBA calculation (see next section), and this was kept as a reference for all the other channels. In the same table a list is also given of the theoretical cross sections for the one-particle transfer channels and of the experimental total cross sections obtained with the time-of-flight spectrometer, where one did not separate the different excited states, but one could integrate the whole transfer flux (including the ground-ground-state transitions).

Most of the transfer products observed before [10] could also be observed in the present experiment. For some nuclei it was not possible to integrate the peaks for several reasons: (1) the nucleus has a complicated level scheme and the transfer flux is fragmented over many transitions (as, e.g., in the case of various odd-odd nuclei), (2) the γ lines overlap with others coming from stronger populated channels, (3) the low-

TABLE I. Integral cross sections for the transfer channels observed in the γ spectra. σ_γ^H and σ_γ^L are the values for the heavy and light partner, respectively. σ_p are from Ref. [10].

	Expt.		Theory		
Channel	σ_γ^H	σ_γ^L	σ^H	σ^L	σ_p
$+1n$	21.71	53.67	55.31	54.85	71.6
$+2n$	20.82	31.33			24.2
$-1p$	39.98	26.53	43.22	32.09	50.8
$-1p+2n$	4.60	1.22			7.3
$-2p$	17.8	22.19			28.5
$-2p+1n$	3.68				10.3
$-2p+2n$	16.72	8.6			6.4
$-2p+3n$	1.62				1.7
$-3p$		2.66			7.9
$-3p-1n$	1.9				2.6
$-3p+2n$	2.77				1.9
$-4p$	3.7				3.2

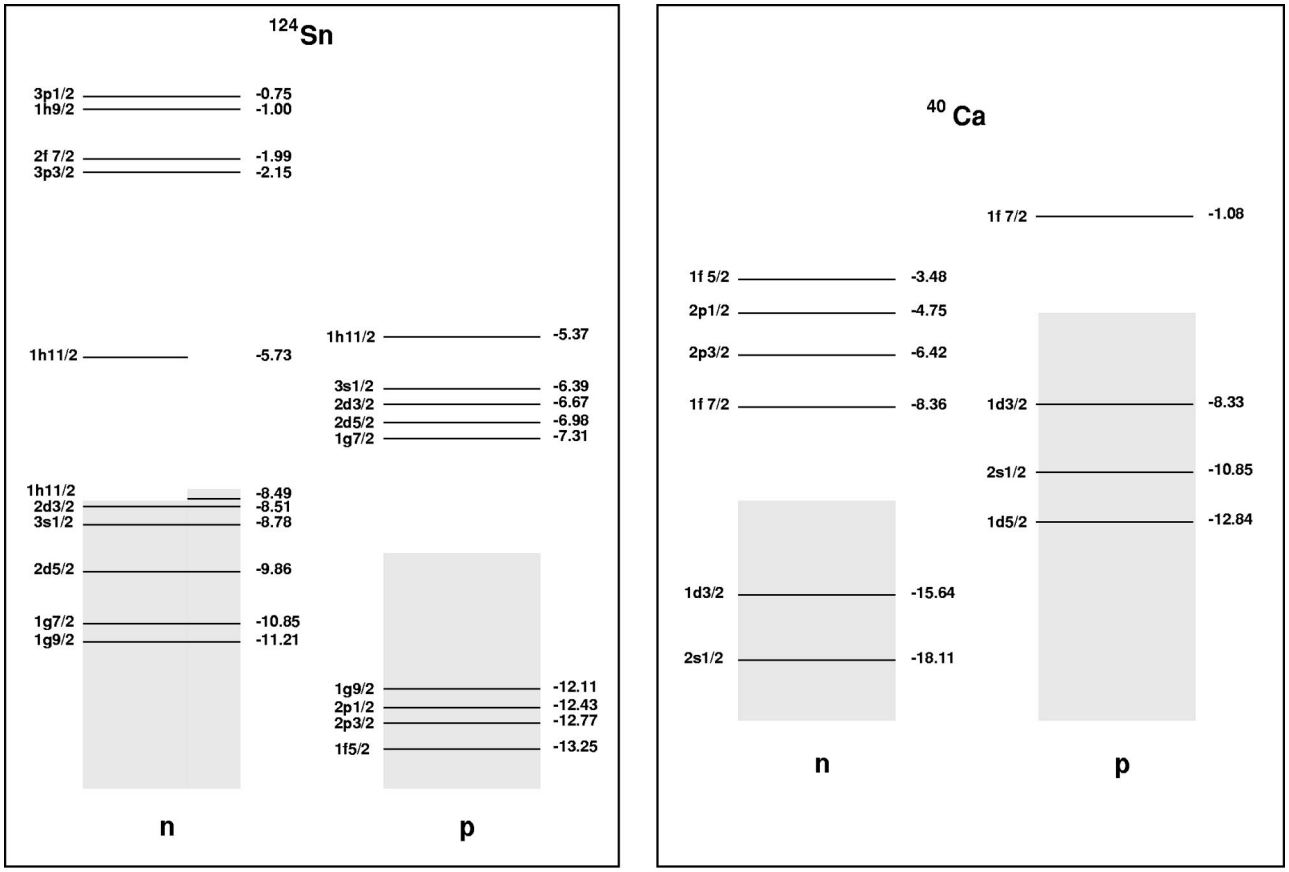

FIG. 7. Single-particle levels of projectile and target used in the calculations. The shaded areas represent the occupied levels. Notice that for the ^{124}Sn this region is not sharp (see text).

est transitions have energies $\leqslant 60$ keV, where the γ-detection efficiency decreases strongly due to the absorption in dead layers and to the thresholds in the electronics, and (4) isomeric states or electron-converted transitions are present.

In discussing the cross sections listed in Table I, one has to keep in mind that in general the lowest or the strongest transition of each observed nucleus might not represent the total transfer flux (this is especially true for odd-even or odd-odd nuclei). Moreover, it is difficult to know experimentally the mutual excitation probability of the light and heavy partners, since the Doppler corrections are different in the two cases. Concerning this last point the GP spectra obtained after gating on a specific transition in a nucleus should show, besides the γ lines belonging to the same nucleus, also those corresponding to the associated partner. We could check this heavy-light cross correlation for the $+1n$ and $-1p$ channels and we estimated a lower limit of 20% for the mutual excitation probability. For channels corresponding to the transfer of two or more nucleons peaks could not be integrated, since, besides the problem of the different Doppler correction, the statistics was a limiting factor.

From Table I, one first notices the very remarkable agreement between the experimental and theoretical values for the $-1p$ and $+1n$ channels (see next section), with the exception of the σ_γ^H of the $+1n$ channel, easily understandable, ^{123}Sn being a nucleus with a very fragmented flux. We feel that the agreement between the present data and those of Ref. [10] is quite reasonable, considering also an average error of 10–20 % in the cross sections for both sets of data.

For channels involving the transfer of at least two nucleons we looked at the GS/GP yield ratio for the various transitions belonging to the same nuclei, and we found that it is rather constant (within an average uncertainty of $\pm 20\%$). The constancy of this ratio means, according to Eq. (1), that the average entry point of the transfer flux lies well above the observed transitions. This is in agreement with the fact that the average excitation energy of the reaction products increases with the number of transferred nucleons [10]. Calculating the contribution of the feeding from higher-lying excited states to the level corresponding to the lowest transitions, one finds the following feeding contributions in the heavy partner: 6% $(+1n)$, 11% $(+2n)$, 51% $(-1p)$, 82% $(-2p)$, and 100% $(-4p)$. For the $-4p$ channel this means a completely negligible direct population to the last level, also in agreement with the previous experiment. For the light partner the trend is quite similar.

IV. COMPARISON WITH CALCULATIONS

We start this section by describing the distorted-Born-wave approximation (DWBA) calculation done with the code FRESCO [31] for the excitation to the lowest 2^+ state in ^{124}Sn, which was used to normalize all the data. In doing so

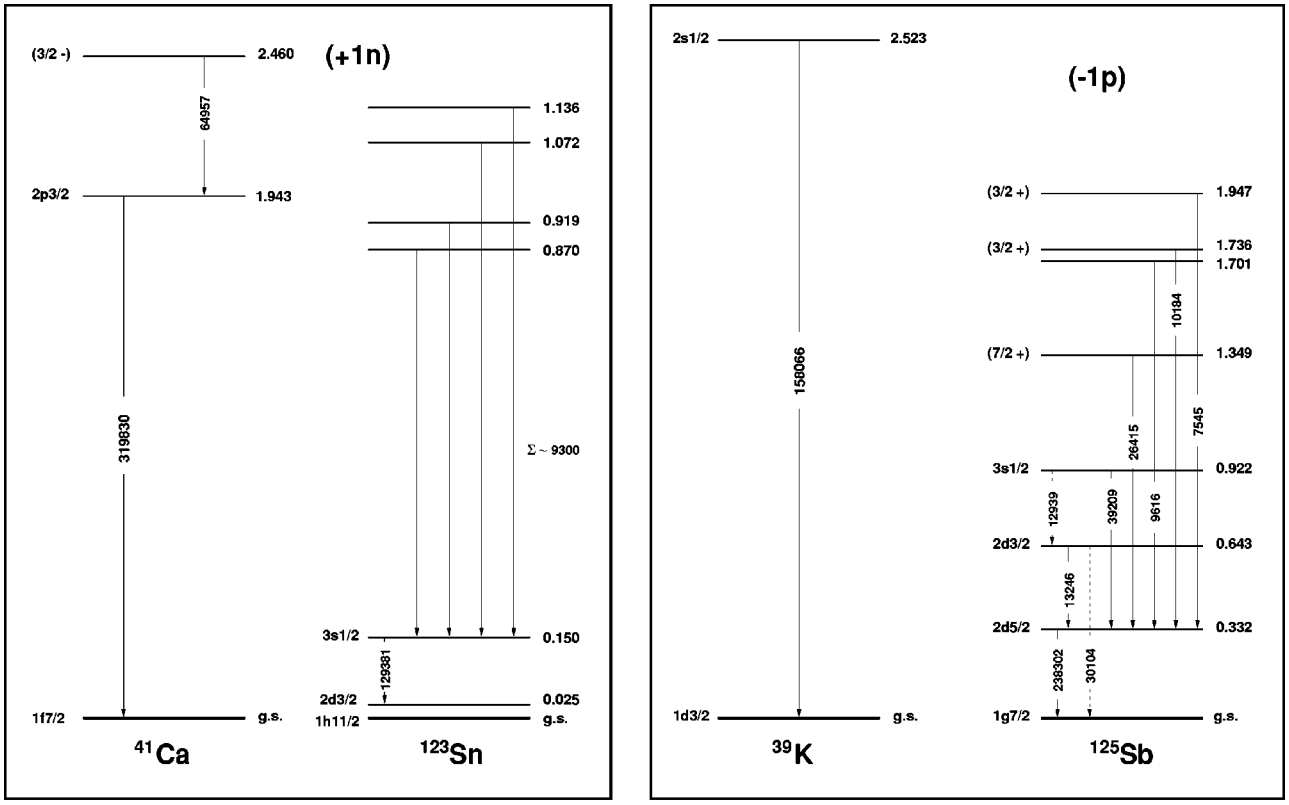

FIG. 8. Transitions and level schemes considered for the analysis of the $(+1n)$ and $(-1p)$ transfer channels. The numbers in parentheses give the experimental total counts for each γ line.

we introduce also the optical potential used in our complex WKB (CWKB) calculations [32] for the transfer channels. This potential is of a standard Woods-Saxon shape whose parameters for the real part have been taken to be $V_0 = -77.27$ MeV, $r_0 = 1.179$ fm and $a_0 = 0.678$ fm, in agreement with the empirical potential of Ref. [33]. The imaginary part has been kept with the same geometry and with a strength $W_0 = -40$ MeV. The corresponding elastic scattering is shown in Fig. 6 (top) in comparison with the quasielastic data of Ref. [10]. At forward angles, our predicted true elastic scattering is in good agreement with the data. The discrepancies at backward angles can be ascribed to the contribution from the excitation of inelastic channels. By using the quoted deformation parameter for the 2^+ state [30] we obtain the cross section of Fig. 6 (bottom) in comparison with the data from the present experiment.

The calculations concerning the transfer processes presented in this section are performed in the CWKB formalism, which is adequate both below and above the Coulomb barrier and which has been successfully applied in the works of Refs. [34,35] to analyze similar reactions. This formalism involves the same approximations which were exploited to calculate the absorptive [36,37] and polarization [38] component of the optical potential and the off-diagonal inelastic couplings [39]. With such a theory one can confidently compute the differential cross sections for the population to specific excited states of the final nuclei produced after the transfer of one particle (in the present case neutron pickup and proton stripping). The above formalism may be generalized [10] to calculate the more complicated multinucleon transfer channels, but only the *Q*-value-integrated cross section can be calculated. Since we do not feel that such a ''global'' analysis is appropriate for these data, we discuss in the following only the one-particle transfer channels.

In the CWKB approximation the cross section for the transfer from the single-particle state $a_i \equiv (n_i, l_i, j_i)$ to the single-particle state $a_f \equiv (n_f, l_f, j_f)$, belonging to different nuclei, may be written as

$$\left[\frac{d\sigma}{d\Omega}\right]_{a_f a_i} = V^2(a_i) U^2(a_f) \sum_{\lambda} \left(\frac{d\sigma}{d\Omega}\right)_{\lambda}, \tag{2}$$

where the sum has to be extended over all the allowed angular momentum transfer λ. The quantity $V^2(a_i)$ represents the probability that the single-particle orbital is occupied, while the quantity $U^2(a_f) = 1 - V^2(a_f)$ is the corresponding probability that the orbital is empty. V^2 and U^2 are directly related to the spectroscopic factors of the single-particle level we are considering.

The transfer cross section for each λ transfer may be written as

$$\left(\frac{d\sigma}{d\Omega}\right)_{\lambda} = \frac{\kappa_f}{\kappa_i} \sum_{\mu} \left| \sum_{l} c_{\lambda\mu}^{a_f a_i}(l) f_l(\theta) \right|^2, \tag{3}$$

where κ_i and κ_f are the asymptotic wave numbers in the entrance and exit channel, respectively, $c_{\lambda\mu}^{a_f a_i}(l)$ is the semi-

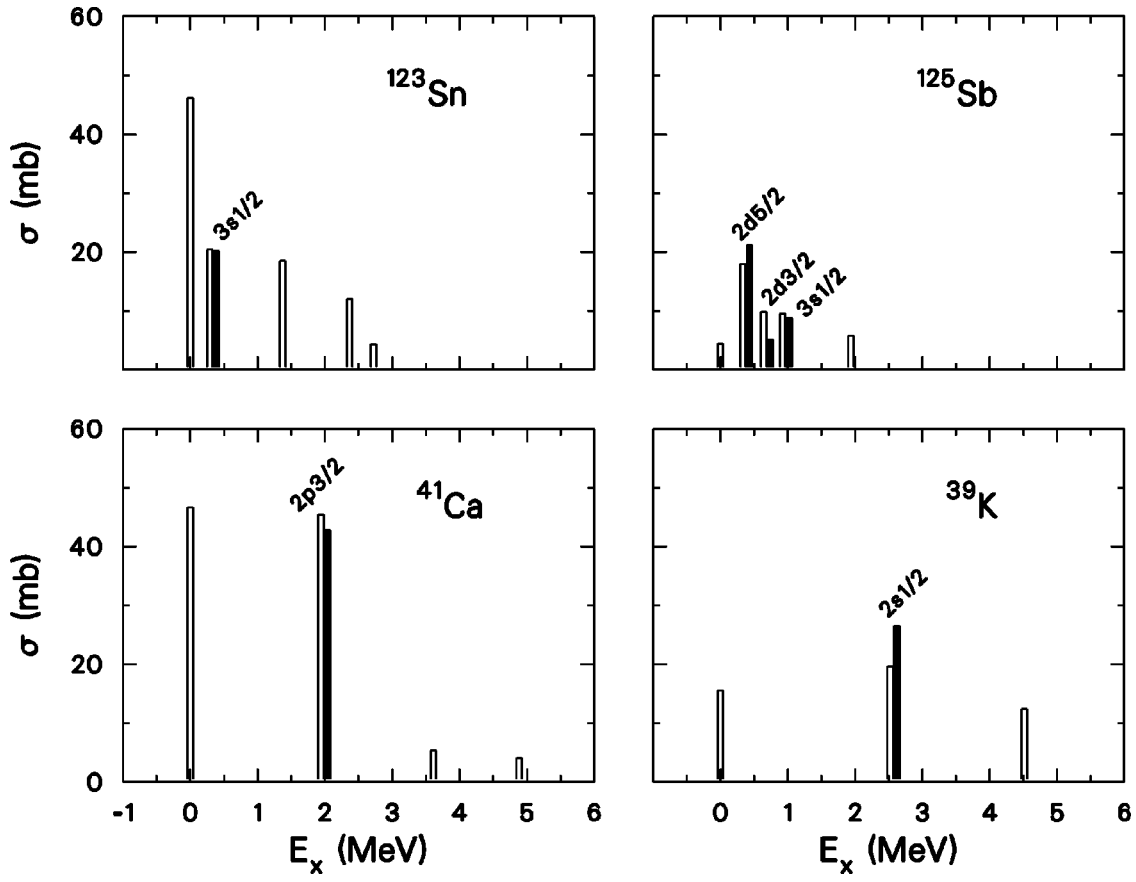

FIG. 9. Experimental (full bars) and theoretical (open bars) total cross sections for the indicated channels. For the ^{123}Sn the line at zero excitation energy includes the population of the metastable state at 24.6 keV. The cross section to this state accounts for more than 80% of the total flux.

classical amplitude for the transition from the initial state a_i to the final state a_f for the partial wave l, and $f_l(\theta)$ is the elastic-scattering amplitude for the same partial wave l.

The transfer amplitude $c_{\lambda\mu}^{a_f a_i}(l)$, in the first-order Born approximation and in the low-recoil limit [36,37], is given by

$$c_{\lambda\mu}^{a_f a_i}(l) = \sqrt{\frac{1}{4\pi\hbar^2}} D_{\mu 0}^{\lambda}\left(0,\frac{\pi}{2},0\right) \times \int_{-\infty}^{+\infty} dt\, f_{\lambda}^{a_f a_i}(r(t)) e^{(i/\hbar)[(\Delta E - Q_{\rm opt} + \Delta)t - \hbar\mu\phi(t)]}. \tag{4}$$

In the above expression $f_{\lambda}^{a_f a_i}(r(t))$ is the single-particle form factor for the transition from the single-particle state a_i to the single-particle state a_f, $Q_{\rm opt}$ is the optimum Q value, and the quantity Δ takes into account the mismatch between the entrance and exit channel trajectories. The time integral has to be performed along the classical trajectory associated to the partial wave l.

The semiclassical amplitudes $c_{\lambda\mu}^{a_f a_i}(l)$ are evaluated in the CWKB approximation by utilizing the single-particle form factors of Refs. [36,37] to which we refer for details. In Fig. 7 we plot the single-particle levels of projectile and target used in the calculations. While for calcium the single-particle levels are well defined, in the case of tin they are only well defined for protons. For neutrons it is in fact more appropriate to talk about quasiparticle and quasihole states, and this is the reason why the $1h_{11/2}$ level appears twice with different energies. The lower level indicates the quasihole energy as extracted from the binding energy of ^{123}Sn, while the top level indicates the energy of the quasiparticle state as extracted from the binding energy of ^{125}Sn. The probability for these quasihole/particle levels to be occupied/unoccupied is indicated by the length representing them being one the full length.

In Fig. 8 we show the levels corresponding to the observed γ lines together with the experimental total counts. To obtain the final cross sections the contribution of the feeding from higher-lying states has been subtracted. Thus, for instance, the cross section for the population of the $2p_{3/2}$ state in ^{41}Ca has been obtained by subtracting the γ intensity of the $3/2^{-}$-$2p_{3/2}$ transition from that of the $2p_{3/2}$ g.s. transition. The extracted cross sections to the individual levels are shown as a function of the excitation energy in Fig. 9 (full bars) compared with the results of our calculation (open bars). The values are also given in Table II. The agreement turns out to be very good, for the transfer channels of both the light and the heavy partners. One can also notice that the calculated ground-ground-state cross sections for both ^{41}Ca and ^{123}Sn represent a substantial fraction of the total flux.

TABLE II. Experimental σ_{exp} and theoretical σ_{th} total transfer cross sections for the indicated one particle transfer channels.

Channel	Nucleus	Level [E (keV)]	σ_{exp} (mb)	σ_{th} (mb)
$-1p$	^{39}K	$2s_{1/2}$ [2522.5]	26.5	19.65
	^{125}Sb	$2d_{5/2}$ [332.1]	21.17	17.99
		$2d_{3/2}$ [643.2]	5.1	9.86
		$3s_{1/2}$ [921.7]	8.75	9.56
$+1n$	^{41}Ca	$2p_{3/2}$ [1942.6]	42.76	45.44
	^{123}Sn	$3s_{1/2}$ [150.4]	20.15	20.40

For ^{123}Sn the bar at the zero excitation energy includes also the metastable state at 24.6 keV, and the transfer to this level accounts for more than 80% of the cross section.

In Fig. 10 we show the theoretical and experimental angular distributions for the direct population of the lowest excited states of the one-particle transfer channels. The experimental cross sections have been obtained by considering θ bins of $\simeq 4°$ in the MWPPAC, and have been derived after subtraction of the feeding from higher-lying excited states. Also shown are the angular distributions for the inclusive cross sections of Ref. [10]. Even in this comparison the agreement between theory and experiment is generally quite good, improvements are possible with a better knowledge of the optical potential (which would require the measurement of pure elastic scattering). The discrepancies present in the inclusive cross sections, especially those of the $+1n$ channel, may indicate an overestimation of the computed ground-ground-state transition yield.

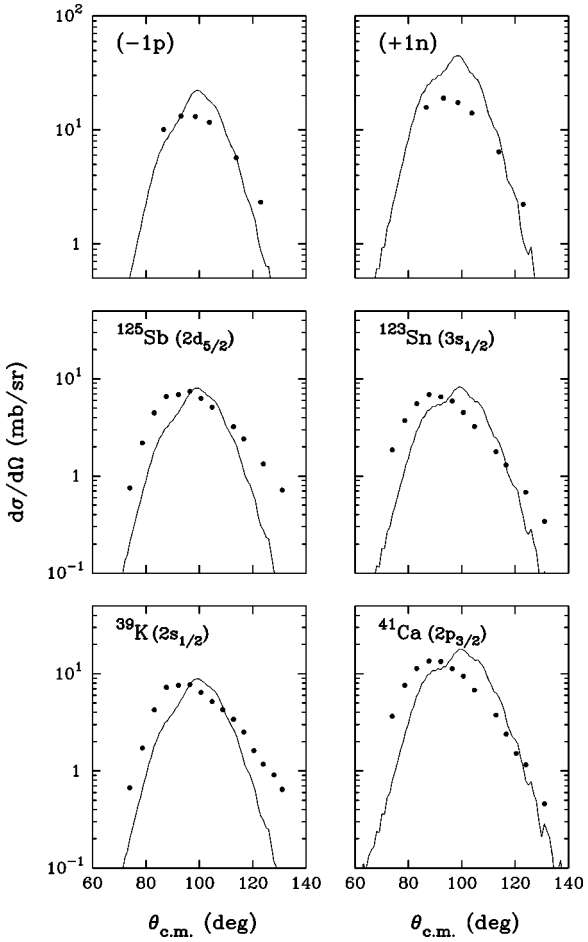

FIG. 10. Center-of-mass angular distributions for the indicated one-particle transfer channels. The experimental angular distributions in the top row are from Ref. [10].

V. CONCLUSIONS

Multinucleon transfer reactions in ^{40}Ca+^{124}Sn at E_{LAB} = 170 MeV have been studied with the GASP γ array coupled to a MWPPAC system. Single and double γ coincidences have been taken for a wealth of transfer channels. The population yield to specific excited states of the transfer reaction products for both the light and heavy partners, and differential and total cross sections have been extracted. A detailed analysis of the one neutron pickup and one-proton stripping has been done by applying the CWKB theory. The comparison of the experimental and theoretical total cross sections shows a remarkably good agreement, demonstrating the correct choice of the form factors and the reliability of the theoretical framework. Finally, γ-γ-particle coincidences have been measured for channels corresponding to the transfer of at least four nucleons. This is useful to plan future experiments to detect the lowest excited states of neutron-rich nuclei, which cannot be produced by other means like via fusion-evaporation reactions.

ACKNOWLEDGMENTS

We acknowledge D. Cline and C.Y. Wu (Rochester) for fruitful discussions on the experiment. We are particularly indebted to C.Y. Wu for providing us with the program of the Doppler corrections and for help in addressing the data analysis. We thank all the members of the GASP Collaboration for precious help during experiments. Thanks also to the LNL accelerator staff for providing us with the good quality ^{40}Ca beam.

[1] C.Y. Wu, W. von Oertzen, D. Cline, and M. Guidry, Annu. Rev. Nucl. Part. Sci. **40**, 285 (1990).
[2] NUPECC Report, ''Nuclear Physics in Europe,'' 1997, edited by J. Vervier *et al.*
[3] W. von Oertzen, H.G. Bohlen, B. Gebauer, R. Künkel, F. Pühlhofer, and D. Schüll, Z. Phys. A **326**, 463 (1987).
[4] R. Künkel, W. von Oertzen, B. Gebauer, H.G. Bohlen, H.A. Bösser, B. Kohlmeyer, F. Pühlhofer, and D. Schüll, Phys. Lett. B **208**, 355 (1988).
[5] J. Speer, W. von Oertzen, D. Schüll, M. Wilpert, H.G. Bohlen, B. Gebauer, B. Kohlmeyer, and F. Pühlhofer, Phys. Lett. B **259**, 422 (1991).
[6] A. Winther, Nucl. Phys. **A572**, 191 (1994).
[7] A. Winther, Nucl. Phys. **A594**, 203 (1995).

[8] C.L. Jiang, K.E. Rehm, J. Gehring, B. Glagola, W. Kutschera, M. Rhein, and A.H. Wuosmaa, Phys. Lett. B **337**, 59 (1994).
[9] C.L. Jiang, K.E. Rehm, H. Esbensen, D.J. Blumenthal, B. Crowell, J. Gehring, B. Glagola, J.P. Schiffer, and A.H. Wuosmaa, Phys. Rev. C **57**, 2393 (1998).
[10] L. Corradi, J.H. He, D. Ackermann, A.M. Stefanini, A. Pisent, S. Beghini, G. Montagnoli, F. Scarlassara, G.F. Segato, G. Pollarolo, C.H. Dasso, and A. Winther, Phys. Rev. C **54**, 201 (1996).
[11] L. Corradi, A.M. Stefanini, J.H. He, C. Lin, S. Beghini, G. Montagnoli, F. Scarlassara, G.F. Segato, G. Pollarolo, C.H. Dasso, and A. Winther, Phys. Rev. C **56**, 938 (1997).
[12] L. Corradi, A.M. Stefanini, C. Lin, S. Beghini, G. Montagnoli, F. Scarlassara, G. Pollarolo, and A. Winther, Phys. Rev. C **59**, 261 (1999).
[13] Proceedings of the International Workshop on ''Heavy-Ion Collisions at Near-Barrier Energies,'' 1997, Canberra (Australia), edited by J. Leigh [J. Phys. G **23**, 1157 (1997)].
[14] M. Dasgupta, D. Hinde, N. Rowley, and A.M. Stefanini, Annu. Rev. Nucl. Part. Sci. **48**, 401 (1998).
[15] D. Bazzacco, Proc. International Conference on ''Nuclear Structure at High Angular Momentum,'' Ottawa (1992), Vol. 2, Proceedings AECL 10613, p. 376
[16] C.W. Beausang and J. Simpson, J. Phys. G **22**, 527 (1996).
[17] R. Broda, B. Fornal, W. Krolas, T. Pawlat, D. Bazzacco, S. Lunardi, C. Rossi Alvarez, R. Menegazzo, G. de Angelis, P. Bednarczyk, J. Rico, D. De Acuna, P.J. Daly, R.H. Mayer, M. Sferrazza, H. Grawe, K.H. Maier, and R. Schubart, Phys. Rev. Lett. **74**, 868 (1995).
[18] B. Fornal, R. Broda, W. Krolas, T. Pawlat, J. Wrzesinski, D. Bazzacco, D. Fabris, S. Lunardi, C. Rossi Alvarez, G. Viesti, G. de Angelis, M. Cinausero, D.R. Napoli, and Z.W. Grabowski, Phys. Rev. C **55**, 762 (1997).
[19] M.W. Guidry, S. Juutinen, X.T. Liu, C.R. Bingham, A.J. Larabee, L.L. Riedinger, C. Baktash, I.Y. Lee, M.L. Halbert, D. Cline, B. Kotlinski, W.J. Kernan, T.M. Semkow, D.G. Saranties, K. Honkanen, and M. Rajagopalan, Phys. Lett. **163B**, 79 (1985).
[20] C.Y. Wu, X.T. Liu, S.P. Sorensen, R.W. Kincaid, M.W. Guidry, D. Cline, W.J. Kernan, E. Vogt, T. Czosnyka, A.E. Kavka, M.A. Stoyer, J.O. Rasmussen, and M.L. Halbert, Phys. Lett. B **188**, 25 (1987).
[21] C.Y. Wu, X.T. Liu, W.J. Kernan, D. Cline, T. Czosnyka, M.W. Guidry, A.E. Kavka, R.W. Kincaid, B. Kotlinski, S.P. Sorensen, and E. Vogt, Phys. Rev. C **39**, 298 (1989).
[22] X.T. Liu, D. Cline, T. Czosnyka, M.W. Guidry, X.L. Han, A.E. Kavka, W.J. Kernan, R.W. Kincaid, S.P. Sorensen, E.G. Vogt, and C.Y. Wu, Phys. Rev. C **43**, R1 (1991).
[23] J. Gerl, W. Korten, W. Habs, D. Schwalm, and H.J. Wollersheim, Z. Phys. A **334**, 195 (1989).
[24] D. Cline, Nucl. Phys. **A520**, 493c (1990).
[25] W.J. Kernan, C.Y. Wu, X.T. Liu, X.L. Han, D. Cline, T. Czosnyka, M.W. Guidry, M.L. Halbert, S. Juutinen, A.E. Kavka, R.W. Kincaid, J.O. Rasmussen, S.P. Sorensen, M.A. Stoyer, and E.G. Vogt, Nucl. Phys. **A524**, 344 (1991).
[26] I. Peter, W. von Oertzen, H.G. Bohlen, A. Gadea, B. Gebauer, J. Gerl, M. Kaspar, I. Kozhoukharov, T. Kröll, M. Rejmund, C. Schlegel, S. Thummerer, H.J. Wollersheim, Eur. Phys. J. A **4**, 313 (1999).
[27] S.J. Sanders, A.K. Dummer, K.A. Farrar, F.W. Prosser, B. Fornal, R.V.F. Janssens, M.P. Carpenter, T.L. Khoo, C. Beck, D. Mahboub, F. Haas, S. Cavallaro, M. Sferrazza, R. Mayer, D. Nisius, and G. de Angelis, Phys. Rev. C **55**, 2541 (1997).
[28] S. Beghini, L. Corradi, J.H. He, and A. dal Bello, Nucl. Instrum. Methods Phys. Res. A **362**, 526 (1995).
[29] A.M. Stefanini *et al.*, International Conference on ''Structure of Nuclei Under Extreme Conditions,'' XVI Nucl. Phys. Div. Conf., EPS, SNEC98, Padova, 1998, edited by S. Lunardi *et al.*, SIF, Editrice Compositori Bologna, p. 895.
[30] R.B. Firestone, *Table of Isotopes*, edited by V. S. Shirley, 8th ed. (Wiley, New York, 1996).
[31] I.J. Thompson, Comput. Phys. Rep. **7**, 167 (1988).
[32] E. Vigezzi and A. Winther, Ann. Phys. (N.Y.) **192**, 432 (1989).
[33] R. Broglia and A. Winther, *Heavy Ion Reactions* (Addison-Wesley, Redwood City, CA, 1991).
[34] D.R. Napoli, A.M. Stefanini, H. Moreno Gonzalez, B. Million, G. Prete, P. Spolaore, M. Narayanasamy, Zi Chang Li, S. Beghini, G. Montagnoli, F. Scarlassara, G.F. Segato, C. Signorini, F. Soramel, G. Pollarolo, and A. Rapisarda, Nucl. Phys. **A559**, 443 (1993).
[35] L. Corradi, A.M. Stefanini, D. Ackermann, S. Beghini, G. Montagnoli, C. Petrache, F. Scarlassara, C.H. Dasso, G. Pollarolo, and A. Winther, Phys. Rev. C **49**, R2875 (1994).
[36] R.A. Broglia, G. Pollarolo, and A. Winther, Nucl. Phys. **A361**, 307 (1981).
[37] G. Pollarolo, R.A. Broglia, and A. Winther, Nucl. Phys. **A406**, 369 (1983).
[38] C.H. Dasso, S. Landowne, G. Pollarolo, and A. Winther, Nucl. Phys. **A459**, 134 (1986).
[39] C.H. Dasso, G. Pollarolo, and S. Landowne, Nucl. Phys. **A443**, 365 (1985).